
Group Equivariant Subsampling

Jin Xu^{1*} Hyunjik Kim² Tom Rainforth¹ Yee Whye Teh^{1,2}

¹ Department of Statistics, University of Oxford, UK.

² DeepMind, UK.

Abstract

Subsampling is used in convolutional neural networks (CNNs) in the form of pooling or strided convolutions, to reduce the spatial dimensions of feature maps and to allow the receptive fields to grow exponentially with depth. However, it is known that such subsampling operations are not translation equivariant, unlike convolutions that *are* translation equivariant. Here, we first introduce translation equivariant subsampling/upsampling layers that can be used to construct exact translation equivariant CNNs. We then generalise these layers beyond translations to general groups, thus proposing *group equivariant subsampling/upsampling*. We use these layers to construct group equivariant autoencoders (GAEs) that allow us to learn low-dimensional equivariant representations. We empirically verify on images that the representations are indeed equivariant to input translations and rotations, and thus generalise well to unseen positions and orientations. We further use GAEs in models that learn object-centric representations on multi-object datasets, and show improved data efficiency and decomposition compared to non-equivariant baselines.

1 Introduction

Convolutional Neural Networks (CNNs) are known to be more data efficient and show better generalisation on perceptual tasks than fully-connected networks, due to translation equivariance encoded in the convolutions: when the input image/feature map is translated, the output feature map also translates by the same amount. In typical CNNs, convolutions are used in conjunction with subsampling operations, in the form of pooling or strided convolutions, to reduce the spatial dimensions of feature maps and to allow receptive field to grow exponentially with depth. Subsampling/upsampling operations are especially necessary for convolutional autoencoders (ConvAEs) [34] because they allow efficient dimensionality reduction. However, it is known that subsampling operations implicit in strided convolutions or pooling layers are *not* translation equivariant [51], hence CNNs that use these components are also not translation invariant. Therefore such CNNs and ConvAEs are not guaranteed to generalise to arbitrarily translated inputs despite their convolutional layers being translation equivariant.

Previous work, such as [3, 51], has investigated how to enforce translation invariance on CNNs, but does not study equivariance with respect to symmetries beyond translations, such as rotations or reflections. In this work, we first describe subsampling/upsampling operations that preserve exact translation equivariance. The main idea is to sample feature maps on an input-dependent grid rather than a fixed one as in pooling or strided convolutions, and the grid is chosen according to a *sampling index* computed from the inputs (see Figure 1). Simply replacing the subsampling/upsampling in standard CNNs with such translation equivariant subsampling/upsampling operations leads to CNNs and transposed CNNs that can map between spatial inputs and low-dimensional representations in a translation equivariant manner.

*Corresponding author: <jin.xu@stats.ox.ac.uk>

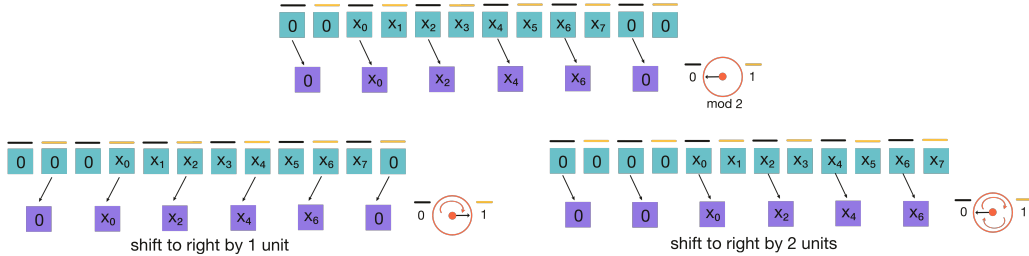


Figure 1: Equivariant subsampling on 1D feature maps with a scale factor $c = 2$. The input feature map has length 8, and initially we sample from odd positions determined by Equation (1) (top). When the original feature map is shifted to the right by 1 unit (bottom left), the sampling index becomes 1, so we instead sample from even positions. When the feature map is shifted to the right by 2 units (bottom right), we again sample from odd positions, but the outputs have been shifted to the right by 1 unit correspondingly.

We further generalise the proposed subsampling/upsampling operations from translations to arbitrary groups, proposing *group equivariant subsampling/upsampling*. In particular we identify subsampling as mapping features on groups G to features on subgroups K (vice versa for upsampling), and identify the sampling index as a coset in the quotient space G/K . See Appendix A for a primer on group theory that is needed to describe this generalisation. We note that group equivariant subsampling is different to *coset pooling* introduced in [5], which instead gives features on the quotient space G/K , and discuss differences in detail in Section 4. Similar to the translation equivariant subsampling/upsampling, group equivariant subsampling/upsampling can be used with group equivariant convolutions to produce group equivariant CNNs. Using such group equivariant CNNs we can construct group equivariant autoencoders (GAEs) that separate representations into an invariant part and an equivariant part.

While there is a growing body of literature on group equivariant CNNs (G-CNNs) [5, 10, 41, 44, 46–48], such equivariant convolutions usually preserve the spatial dimensions of the inputs (or lift them to even higher dimensions) until the final invariant pooling layer. There is a lack of exploration on how to reduce the spatial dimensions of such feature maps while preserving exact equivariance, to produce low-dimensional equivariant representations. This work attempts to fill in this gap. Such low-dimensional equivariant representations can be employed in representation learning methods, allowing various advantages such as interpretability, out-of-distribution generalisation, and better sample complexity. When using such learned representations in downstream tasks such as abstract reasoning, reinforcement learning, video modelling, scene understanding, it is especially important for representations to be equivariant rather than invariant in these tasks, because transformations and how they act on feature spaces are critical information, rather than nuisance as in image classification problems.

In summary, we make the following contributions: (i) We propose subsampling/upsampling operations that preserve translational equivariance. (ii) We generalise the proposed subsampling/upsampling operations to arbitrary symmetry groups. (iii) We use equivariant subsampling/upsampling operations to construct GAEs that gives low-dimensional equivariant representations. (iv) We empirically show that representations learned by GAEs enjoys many advantages such as interpretability, out-of-distribution generalisation, and better sample complexity.

2 Equivariant Subsampling and Upsampling

2.1 Translation Equivariant Subsampling for CNNs

In this section we describe the proposed translation equivariant subsampling scheme for feature maps in standard CNNs. Later in Section 2.2, we describe how this can be generalised to group equivariant subsampling for feature maps on arbitrary groups.

Standard subsampling Feature maps in CNNs can be seen as functions defined on the integer grid, e.g. \mathbb{Z} for 1D feature maps, and \mathbb{Z}^2 for 2D. Hence we represent feature maps as $f : \mathbb{Z} \rightarrow \mathbb{R}^d$, where d is the number of feature map channels. For simplicity, we start with 1D and move on to the 2D case. Typically, subsampling in CNNs is implemented as either strided convolution or (max)

pooling, and they can be decomposed as

$$\begin{aligned}\text{CONV}_k^c &= \text{SUBSAMPLING}^c \circ \text{CONV}_k^1 \\ \text{MAXPOOL}_k^c &= \text{SUBSAMPLING}^c \circ \text{MAXPOOL}_k^1\end{aligned}$$

where subscripts denote kernel sizes and superscripts indicate strides. $c \in \mathbb{N}$ is the scale factor for SUBSAMPLING, and this operation simply restricts the input domain of the feature map from \mathbb{Z} to $c\mathbb{Z}$, without changing the corresponding function values.

Translation equivariant subsampling In our equivariant subsampling scheme, we instead restrict the input domain to $c\mathbb{Z} + i$, the integers $\equiv i \pmod{c}$, where i is a sampling index determined by the input feature map. The key idea is to choose i such that it shifts by $t \pmod{c}$ when the input is translated by t , to ensure that the same features are subsampled upon translation. Let i be given by the mapping $\Phi_c : \mathcal{I}_{\mathbb{Z}} \rightarrow \mathbb{Z}/c\mathbb{Z}$. $\mathcal{I}_{\mathbb{Z}}$ denotes the space of vector functions on \mathbb{Z} and $\mathbb{Z}/c\mathbb{Z}$ is the space of remainders upon division by c .

$$i = \Phi_c(f) = \text{mod}(\arg \max_{x \in \mathbb{Z}} \|f(x)\|_1, c) \quad (1)$$

where $\|\cdot\|_1$ denotes L^1 -norm (other choices of norm are equally valid). Other choices for Φ_c are equally valid as long as they satisfy translation equivariance, ensuring that the same features are subsampled upon translation of the input:

$$\Phi_c(f(\cdot - t)) = \text{mod}(\Phi_c(f) + t, c). \quad (2)$$

Note that this holds for Equation (1) provided the argmax is unique, which we assume for now (see Appendix B.1 for a discussion of the non-unique case). We can decompose the subsampled feature map defined on $c\mathbb{Z} + i$ into its values and the offset index i , expressing it as $[f_b, i] \in (\mathcal{I}_{c\mathbb{Z}}, \mathbb{Z}/c\mathbb{Z})$, where f_b is the translated output feature map such that $f_b(cx) = f(cx + i)$ for $x \in \mathbb{Z}$.

The subsampling operation described above, which maps from $\mathcal{I}_{\mathbb{Z}}$ to $(\mathcal{I}_{c\mathbb{Z}}, \mathbb{Z}/c\mathbb{Z})$ is translation equivariant: when the feature map f is translated to the right by $t \in \mathbb{Z}$, one can verify that f_b will be translated to the right by $c \lfloor \frac{i+t}{c} \rfloor$, and the sampling index for the translated inputs would become $\text{mod}(i + t, c)$. We provide an illustration for $c = 2$ in Figure 1, and describe formal statements and proofs later for the general cases in Section 2.2.

Multi-layer case For the subsequent layers, the feature map f_b is fed into the next convolution, and the sampling index i is appended to a list of outputs. When the above translation equivariant subsampling scheme is interleaved with convolutions in this way, we obtain an exactly translation equivariant CNN, where each subsampling layer with scale factor c_k produces a sampling index $i_k \in \mathbb{Z}/c_k\mathbb{Z}$. Hence the equivariant representation output by the CNN with L subsampling layers is a final feature map f_L and a L -tuple of sampling indices (i_1, \dots, i_L) . This tuple can in fact be expressed equivalently as a single integer by treating the tuple as mixed radix notation and converting to decimal notation. We provide details of this multi-layer case in Appendix B.2, including a rigorous formulation and its equivariance properties.

Translation equivariant upsampling As a counterpart to subsampling, upsampling operations increase the spatial dimensions of feature maps. We propose an equivariant upsampling operation that takes in a feature map $f \in \mathcal{I}_{c\mathbb{Z}}$ and a sampling index $i \in \mathbb{Z}/c\mathbb{Z}$, and outputs a feature map $f_u \in \mathcal{I}_{\mathbb{Z}}$, where we set $f_u(cx + i) = f(cx)$ and $\mathbf{0}$ everywhere else. This works well enough in practice, although in conventional upsampling the output feature map is often a smooth interpolation of the input feature map. To achieve this with equivariant upsampling, we can additionally apply average pooling with stride 1 and kernel size > 1 .

2D Translation equivariant subsampling When feature maps are $2D$, they can be represented as functions on \mathbb{Z}^2 . The sampling index becomes a 2-element tuple given by:

$$\begin{aligned}(x^*, y^*) &= \arg \max_{(x,y) \in \mathbb{Z}^2} \|f(x)\|_1 \\ (i, j) &= (\text{mod}(x^*, c), \text{mod}(y^*, c))\end{aligned}$$

and we subsample feature maps by restricting the input domain to $c\mathbb{Z}^2 + (i, j)$. The multi-layer construction and upsampling is analogous to the 1D-case.

2.2 Group Equivariant Subsampling and Upsampling

In this section, we propose group equivariant subsampling by starting off with the 1D-translation case in Section 2.1, and provide intuition for how each component of this special case generalises to arbitrary discrete groups G . We then proceed to mathematically formulate group equivariant subsampling, and prove that it is indeed G -equivariant.

Feature maps on groups First recall that the feature maps for the 1D-translation case were defined as functions on \mathbb{Z} , or $f \in \mathcal{I}_{\mathbb{Z}}$ for short. To extend this to the general case, we consider feature maps f as functions on a group G , i.e. $f \in \mathcal{I}_G = \{f : G \rightarrow V\}^2$ where V is a vector space, as is done in e.g. group equivariant CNNs (G-CNNs) [5]. Note that translating feature maps f on \mathbb{Z} by displacement u is effectively defining a new feature map $f'(\cdot) = f(\cdot - u)$. In the general case, we say that the group action on the feature space is given by

$$[\pi(u)f](g) = f(u^{-1}g) \quad (3)$$

where π is a group representation describing how $u \in G$ acts on the feature space.

Recap: translation equivariant subsampling Recall that standard subsampling that occurs in pooling or strided convolutions for 1D translations amounts to restricting the domain of the feature map from \mathbb{Z} to $c\mathbb{Z}$, whereas equivariant subsampling also produces a sampling index $i \in \mathbb{Z}/c\mathbb{Z}$, an integer mod c , and that this is equivalent to restricting the input domain to $c\mathbb{Z} + i$. i is given by the translation equivariant mapping $\Phi_c : \mathcal{I}_{\mathbb{Z}} \rightarrow \mathbb{Z}/c\mathbb{Z}$. We can translate the input domain back to $c\mathbb{Z}$, and represent the output of subsampling as $[f_b, i] \in (\mathcal{I}_{c\mathbb{Z}}, \mathbb{Z}/c\mathbb{Z})$, where f_b is the translated output feature map and $f_b(cx) = f(cx + i)$ for $x \in \mathbb{Z}$.

Group equivariant subsampling Similarly in the general case, for a feature map $f \in \mathcal{I}_G$, standard subsampling can be seen as restricting the domain from the group G to a subgroup K , whereas equivariant subsampling additionally produces a sampling index $pK \in G/K$, where the quotient space $G/K = \{gK : g \in G\}$ is the set of (left) *cosets* of K in G . Note that we have rewritten i as p to distinguish between the 1D translation case and the general group case. This is equivalent to restricting the f to the coset pK . The choice of the coset pK is given by equivariant map $\Phi : \mathcal{I}_G \rightarrow G/K$ (the action of G on G/K is given by $u(gK) = (ug)K$ for $u, g \in G$), such that $pK = \Phi(f)$. This restriction of f to pK can also be thought of as having an output feature map f_b on K and choosing a coset representative element $\bar{p} \in pK$, such that $f_b(k) = f(\bar{p}k)$. This choice of coset representative is described by a function $s : G/K \rightarrow G$, such that $\bar{p} = s(pK)$. The function s is called a section and should satisfy $s(pK)K = pK$.

Now let us formulate subsampling and upsampling operations $S_b \downarrow_K^G$ and $S_u \uparrow_K^G$ mathematically and prove its G -equivariance. Let $\mathcal{I}_K = \{f : K \rightarrow V\}$ be the space of feature map on K . $S_b \downarrow_K^G$ takes in a feature map $f \in \mathcal{I}_G$ and produces a feature map $f_b \in \mathcal{I}_K$ and a coset in G/K . In reverse, the upsampling operation $S_u \uparrow_K^G$ takes in a feature map in \mathcal{I}_K , a coset in G/K , and produces a feature map in \mathcal{I}_G . We use a section $s : G/K \rightarrow G$ to represent a coset with a representative element in G , and point out that equivariance holds for any choice of s .

Formally, given an equivariant map $\Phi : \mathcal{I}_G \rightarrow G/K$ (we will discuss how to construct such a map in Section 2.3), and a fixed section $s : G/K \rightarrow G$ such that $\bar{p} = s(pK)$, the subsampling operation $S_b \downarrow_K^G : \mathcal{I}_G \rightarrow \mathcal{I}_K \times G/K$ is defined as:

$$\begin{aligned} pK &= \Phi(f), \quad f_b(k) = f(\bar{p}k) \text{ for } k \in K \\ [f_b, pK] &= S_b \downarrow_K^G(f; \Phi), \end{aligned} \quad (4)$$

while the upsampling operation $S_u \uparrow_K^G : \mathcal{I}_K \times G/K \rightarrow \mathcal{I}_G$ is defined as:

$$\begin{aligned} f_u(g) &= f(\bar{p}^{-1}g) \text{ if } g \in K \text{ else } \mathbf{0} \\ f_u &= S_u \uparrow_K^G(f, pK). \end{aligned} \quad (5)$$

²This is not to be confused with the space of Mackey functions in, e.g., [9], and rather it is the space of unconstrained functions on G .

To make the output of the upsampling dense rather than sparse, one can apply arbitrary equivariant smoothing functions such as average pooling with stride 1 and kernel size > 1 , to compensate for the fact that we extend with 0s rather than values close to their neighbours. In practice, we observe that upsampling without any smoothing function works well enough.

The statement on the equivariance of $S_b \downarrow_K^G$ and $S_u \uparrow_K^G$ requires we specify the action of G on the space $\mathcal{I}_K \times G/K$, which we denote as π' . For any $u \in G$,

$$\begin{aligned} p'K &= upK, & f'_b &= \pi(\bar{p}'^{-1}u\bar{p})f_b \\ [f'_b, p'K] &= \pi'(u)[f_b, pK] \end{aligned} \quad (6)$$

Lemma 2.1. π' defines a valid group action of G on the space $\mathcal{I}_K \times G/K$.

We can now state the following equivariance property (See Appendix D for a proof):

Proposition 2.2. *If the action of group G on the space \mathcal{I}_G and $\mathcal{I}_K \times G/K$ are specified by π, π' (as defined in Equations (3) and (6)), and $\Phi : \mathcal{I}_G \rightarrow G/K$ is an equivariant map, then the operations $S_b \downarrow_K^G$ and $S_u \uparrow_K^G$ as defined in Equations (4) and (5) are equivariant maps between \mathcal{I}_G and $\mathcal{I}_K \times G/K$.*

2.3 Constructing Φ

We use the following simple construction of the equivariant mapping $\Phi : \mathcal{I}_G \rightarrow G/K$ for subsampling/upsampling operations, although any equivariant mapping would suffice. For an input feature map $f \in \mathcal{I}_G$, we define

$$pK = \Phi(f) := (\arg \max_{g \in G} \|f(g)\|_1)K \quad (7)$$

Provided that the argmax is unique, it is easy to show that $(up) \cdot K = \Phi(\pi(u)f)$, hence Φ is equivariant. In practice one can insert arbitrary equivariant layers to f before and after we take the norm $\|\cdot\|_1$ to avoid a non-unique argmax (see Appendix E).

In theory, there could exist cases where the argmax is always non-unique. We provide a more complex construction of Φ that deals with this case in Appendix B.1.

3 Application: Group Equivariant Autoencoders

Group equivariant autoencoders (GAEs) are composed of alternating G-convolutional layers and equivariant subsampling/upsampling operations for the encoder/decoder. One important property of GAEs is that the final subsampling layer of the encoder subsamples to a feature map defined on the trivial group $\{e\}$, outputting a vector (instead of a feature map) that is *invariant*. For the 1D-translation case, suppose the input to the final subsampling layer is a feature map f defined on \mathbb{Z} . Then the final layer produces an invariant vector $f_b(0) = f(i_L)$ where $i_L = \arg \max_{x \in \mathbb{Z}} \|f(x)\|_1$. Note that there is no scale factor c_L here. Intuitively we can think of this as setting the scale factor $c_L = \infty$. Hence the encoder of the GAE outputs a representation that is disentangled into an invariant part $z_{\text{inv}} = f_b(0)$ (the vector output by the final subsampling layer) and an equivariant part $z_{\text{eq}} = (i_1, \dots, i_L)$.

For the general group case, instead of specifying scale factors as in Section 2.1, we specify a sequence of nested subgroups $G = G_0 \geq G_1 \geq \dots \geq G_L = \{e\}$, where the feature map for layer l is defined on subgroup G_L . For example, for the $p4$ group $G = \mathbb{Z} \rtimes C_4$, we can use the following sequence for subsampling: $\mathbb{Z} \rtimes C_4 \geq 2\mathbb{Z} \rtimes C_4 \geq 4\mathbb{Z} \rtimes C_4 \geq 8\mathbb{Z} \rtimes C_2 \geq \{e\}$. Note that for the final two layers of this example, we are subsampling translations and rotations jointly.

We lift the input defined on the homogeneous input space to \mathcal{I}_G (see Appendix A.3 for details on homogeneous spaces and lifting), and treat $f_0 \in \mathcal{I}_G$ as inputs to the autoencoders. The group equivariant encoder ENC can be described as follows:

$$\begin{aligned} [f_l, p_l G_l] &= S_b \downarrow_{G_l}^{G_{l-1}} (\text{G-CNN}_{l-1}^E(f_{l-1}); \Phi_l) \\ [z_{\text{inv}}, z_{\text{eq}}] &= [f_L(e), (p_1 G_1, p_2 G_2, \dots, p_L G_L)] \end{aligned} \quad (8)$$

where $l = 1, \dots, L$ and $\text{G-CNN}_l(\cdot)$ denotes G-convolutional layers before the l th subsampling layer.

The decoder DEC simply goes in the opposite direction, and can be written formally as:

$$f_L \text{ is defined on } G_L = \{e\} \text{ and } f_L(e) = z_{\text{inv}}$$

$$f_{l-1} = \text{G-CNN}_{l-1}^D(S_u \uparrow_{G_l}^{G_l} (f_l, p_l G_l)) \quad (9)$$

where $l = L, \dots, 1$ and $\hat{f} = f_0$ gives the final reconstruction.

Recall from Section 2.1 that the tuple (i_1, \dots, i_L) can be expressed equivalently as a single integer. Similarly, the tuple $(p_1 G_1, p_2 G_2, \dots, p_L G_L)$ can be expressed as a single group element in G . We show in Appendix B.2 that the action implicitly defined on the tuple via Equation (6) simplifies elegantly to the left-action on the single group element in G .

We now have the following properties for the learned representations (see Appendix D for a proof):

Proposition 3.1. *When ENC and DEC are given by Equations (8) and (9), and the group actions are specified as in Equation (3) and Equation (6), for any $g \in G$ and $f \in \mathcal{I}_G$, we have*

$$[z_{\text{inv}}, g \cdot z_{\text{eq}}] = \text{ENC}(\pi(g)f)$$

$$\pi(g)\hat{f} = \text{DEC}(z_{\text{inv}}, g \cdot z_{\text{eq}})$$

4 Related Work

Group equivariant neural networks The equivariant subsampling/upsampling that we propose deals with feature maps (functions) defined on the space of the group G or its subgroups K , which transform under the *regular representation* with the group action. Hence our equivariant subsampling/upsampling is compatible with *lifting-based* group equivariant neural networks defined on discrete groups [5, 22, 37, 38] that define a mapping between feature maps on G . We also discuss the extension of group equivariant subsampling to be compatible with those defined on continuous/Lie groups [1, 6, 14, 16, 24] in Section 6. This is in contrast to group equivariant neural networks that do not use lifting and use *irreducible representations*, defining mappings between feature maps on the input space \mathbf{X} . [10, 15, 17, 30, 41, 44, 46–48].

Coset pooling In particular, [5] propose *coset pooling*, which is also a method for equivariant subsampling. Here a feature map f on G is mapped onto a feature map $\Phi(f)$ on G/K (as opposed to K , for our equivariant subsampling) as follows:

$$\Phi(f)(gK) = \text{POOL}_{k \in K} f(gk) \quad (10)$$

such that the feature values on the coset gK are pooled. For the 1D-translation case, where $G = \mathbb{Z}$, $K = c\mathbb{Z}$, this amounts to pooling over every c th pixel, which disrupts the locality of features as opposed to our equivariant subsampling that preserves locality, and hence is more suitable to use with convolutions for translation equivariance. See Figure 2 for a visual comparison. As such, the $p4$ -CNNs in [5] use standard max pooling with stride=2 rather than coset pooling for \mathbb{Z}^2 , and coset-pooling is only used in the final layer to pool over feature maps across 90-degree rotations, achieving exact rotation equivariance but imperfect translation equivariance. In our work, we use translation equivariant subsampling in the earlier layers and rotation equivariant subsampling in the final layers to achieve exact roto-translation equivariance.

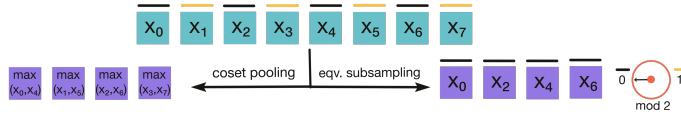


Figure 2: Coset (max) pooling vs. equivariant subsampling.

Unsupervised disentangling and object discovery GAEs produce equivariant (z_{eq}) and invariant (z_{inv}) representations, effectively separating position and pose information with other semantic information. This relates to unsupervised disentangling [4, 21, 28, 52] where different factors of variation in the data are separated in different dimensions of a low-dimensional representation. However unlike equivariant subsampling, there is no guarantee of any equivariance in the low-dimensional representation, making the resulting disentangled representations less interpretable. Works on unsupervised object discovery [2, 13, 19, 32] learn object-centric representations, and we showcase GAEs in MONet [2] where we replace their VAE with a V-GAE in order to separate position and pose information and learn more interpretable representations of objects in a data-efficient manner.

Shift-invariance in CNNs As early as [40], it has been discussed that shift-invariance cannot hold for conventional subsampling. Although standard subsampling operations such as pooling or strided convolutions are not *exactly* shift invariant, they do not prevent strong performance on classification tasks [39]. Nonetheless, [51] integrates anti-aliasing to improve shift-invariance, showing that it leads to better performance and generalisation on classification tasks. [3] explore a similar strategy to our equivariant subsampling by partitioning feature maps into polyphase components and select the component with the highest norm. However, unlike the proposed group equivariant subsampling/upsampling which tackle general equivariance for arbitrary discrete groups, both works focus only on translation invariance.

5 Experiments

In this section, we compare the performance of GAEs with equivariant subsampling to their non-equivariant counterparts that use standard subsampling/upsampling in object-centric representation learning. We show that GAEs give rise to more interpretable representations that show better sample complexity and generalisation than their non-equivariant counterparts.

Models and Baselines (G-)Convolutional autoencoders (G)ConvAE are composed of alternating (G-)convolutional layers and subsampling/upsampling operations with a final MLPs applied to the flattened feature maps. We categorize models by the types of equivariance preserved by the convolutional layers. We consider three different discrete symmetry groups: $p1$ (only translations), $p4$ (composition of translations and 90 degree rotations), $p4m$ (composition of translations, 90 degree rotations and mirror reflection). The baseline models are: ConvAE- $p1$ (standard convolutional autoencoders), GConvAE- $p4$, GConvAE- $p4m$, where the corresponding equivariance is preserved in the (G-)convolutional layers but not in the subsampling/upsampling operations. The equivariant counterparts of these baseline models are GAE- $p1$, GAE- $p4$, GAE- $p4m$, where the subsampling/upsampling operations are also equivariant. For baseline models, we use a scale factor of 2 for all subsampling/upsampling layers. For GAEs, we subsample first the translations, then rotations, followed by reflections, all with scale factor 2. e.g. for GAE- $p4m$, the feature maps at each layer are defined on the following chain of nested subgroups: $\mathbb{Z}^2 \times (C_4 \times C_2) \geq (2\mathbb{Z})^2 \times (C_4 \times C_2) \geq (4\mathbb{Z})^2 \times (C_4 \times C_2) \geq (8\mathbb{Z})^2 \times (C_4 \times C_2) \geq (16\mathbb{Z})^2 \times (C_2 \times C_2) \geq \{e\}$. As in [5], we rescale the number of channels such that the total number of parameters of these models roughly match each other.

Data To demonstrate basic properties of GAEs and compare sample complexity under the single object scenario, we use Colored-dSprite [35] and a modification of FashionMNIST [49], where we first apply zero-padding to reach a size of 64×64 , followed by random shifts, rotations and coloring. For multi-object datasets, we use Multi-dSprites [26] and CLEVR6 which is a variant of CLEVR [25] with up to 6 objects. All input images are resized to a resolution of 64×64 .

See Appendix E and our reference implementation³ for more details on hyperparameters and data preprocessing. Our implementation is built upon open source projects [13, 20, 23, 36, 42, 45, 50].

5.1 Basic Properties: Equivariance, Disentanglement and Out-of-Distribution Generalization

Equivariance The encoder-decoder pipeline in GAEs is exactly equivariant. In Figure 3, we train GAE- $p4m$ on 6400 examples from Colored-dSprites, and we show how to manipulate reconstructions by manipulating the equivariant representation z_{eq} (left). If an image x is encoded into $[z_{inv}, z_{eq}]$, then decoding $[z_{inv}, g \cdot z_{eq}]$ will give $g \cdot \hat{x}$ where \hat{x} is the reconstruction of x .

Disentanglement The learned representations in GAEs are disentangled into an invariant part z_{inv} and an equivariant part z_{eq} . In Figure 3 (left), we vary the equivariant part while the invariant part remains the same. In Figure 3 (right), we show the frames of a movie of a heart, and show its reconstruction after replacing z_{inv} representing a heart with that of an ellipse. Note that the ellipse shape undergoes the same sequence of transformations as the heart.

Out-of-distribution generalisation GAEs can generalise to data with unseen object locations and poses. We train an GAE- $p4$ on 6400 constrained training examples, where we only use examples

³<https://github.com/jinxu06/gsubsampling>

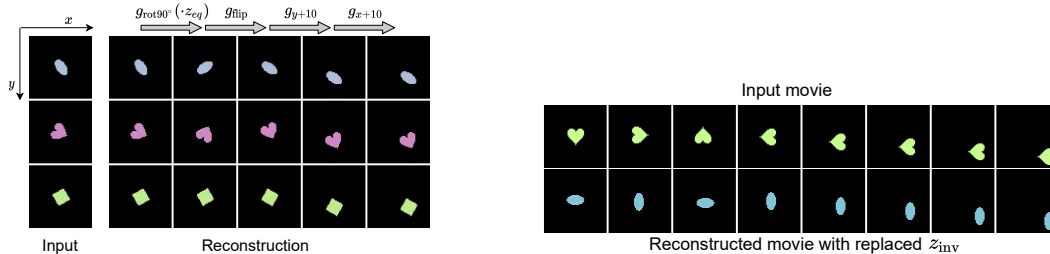


Figure 3: (Left) Manipulating reconstructions by modifying the equivariant part z_{eq} . The second column are the original reconstructions, which match the inputs well. The subsequent columns are reconstructions decoded from modified z_{eq} . We transform z_{eq} with a sequence of group elements, and show the resulting reconstructions. (Right) Manipulating reconstruction shape by modifying z_{inv} .

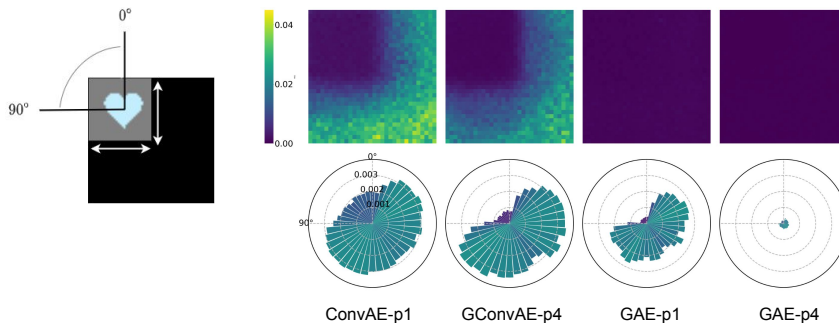


Figure 4: Generalisation to out-of-distribution object locations and poses. During training, we constrain shapes to be in the top-left quarter, and the orientation to be always less than 90 degrees. On the right, we compare the error of reconstructions of different models generalise on objects at unseen locations in the first row, and how they generalise to unseen orientations in the second row.

with locations in the top-left quarter and orientations within $[0, 90]$ degrees, as shown in Figure 4. During test time, we evaluate mean squared error (MSE) of reconstructions on unfiltered test data to see how models generalise to unseen location and poses. Both ConvAE- $p1$ and GConvAE- $p4$ cannot generalise well to object poses out of their training distribution. In contrast, GAE- $p1$ generalise to any locations without performance degradation but not to unseen orientations, while GAE- $p4$, which encodes both translation and rotation equivariance, generalises well to all locations and orientations. We only use heart shapes for evaluation, because the square and ellipse have inherent symmetries.

5.2 Single Object

Since GAEs are fully equivariant and can generalize to unseen object poses, it is natural to conjecture that such models can significantly improve data efficiency when symmetry-transformed data points are also plausible samples from the data distribution. We test this hypothesis on Colored-dSprites and transformed FashionMNIST, and the results are shown in Figure 5. On both datasets, equivariant autoencoders significantly outperform their non-equivariant counterparts for all considered training set sizes. In fact, as shown in the figure, equivariant models trained with a smaller training set size is often comparable to baseline models trained on a larger training set. Furthermore, the results demonstrate that it is beneficial to consider symmetries beyond translations in these problems: for both non-equivariant and equivariant models, variants that encode rotation and reflection symmetries consistently show better performance compared to models that only consider the translation symmetry.

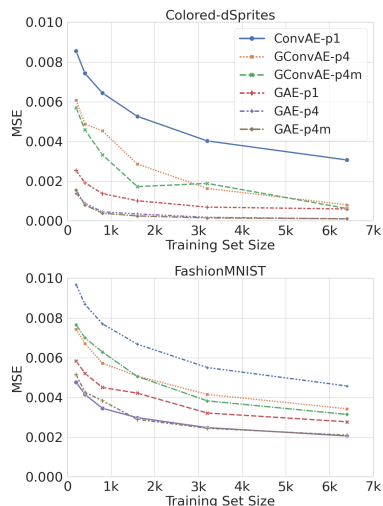


Figure 5: Reconstruction error on single object datasets

Table 1: Reconstruction error MSE ($\times 10^{-3}$) (mean(stddev) across 5 seeds) on multi-object datasets

Dataset	Multi-dSprites			CLEVR6		
Training Set Size	3200	6400	12800	3200	6400	12800
MONet	2.661(0.382)	1.385(0.235)	0.326(0.076)	0.673(0.059)	0.562(0.057)	0.546(0.056) ¹
MONet-GAE- <i>p</i> 1	0.659(0.103)	0.359(0.025)	0.264(0.042)	0.473(0.064)	0.432(0.052)	0.388(0.016)
MONet-GAE- <i>p</i> 4	0.563(0.195)	0.317(0.060)	0.231(0.067)	0.461(0.025)	0.414(0.022)	0.413(0.018)

Table 2: Foreground segmentation performance in terms of ARI (mean(stddev) across 5 seeds)

Dataset	Multi-dSprites			CLEVR6		
Training Set Size	3200	6400	12800	3200	6400	12800
MONet	0.597(0.022)	0.747(0.049)	0.891(0.009)	0.829(0.055)	0.878(0.023)	0.865(0.033) ¹
MONet-GAE- <i>p</i> 1	0.762(0.049)	0.823(0.042)	0.889(0.013)	0.921(0.015)	0.917(0.032)	0.920(0.025)
MONet-GAE- <i>p</i> 4	0.753(0.089)	0.833(0.072)	0.902(0.025)	0.878(0.055)	0.914(0.012)	0.910(0.011)

¹ We excluded 2 outliers here as the baseline MONet occasionally fails during late-phase training.

5.3 Multiple Objects

In multi-object scenes, it is often more interesting to consider local symmetries associated with objects rather than the global symmetry for the whole image. To exploit object symmetries in image data, one needs to first discover objects and separate them from the background, which is a challenging problem on its own. Currently, GAEs do not have inherent capability to solve these problems. In order to investigate whether our models could improve data efficiency in multi-object settings, we rely on recent work on unsupervised object discovery and only use GAEs to model object components. More specifically, we explored replacing component VAEs in MONet [2] with V-GAEs (probabilistic version of our GAEs, where a standard Gaussian prior is put on z_{inv} and z_{eq} remains deterministic), and train models end-to-end. Again we study the low data regime to show results on data efficiency.

We train models on Multi-dSprites and CLEVR6 with training set sizes 3200, 6400 and 12800. We consider two evaluation metrics: mean squared error (MSE) to measure the overall reconstruction quality, and adjusted rand index (ARI), which is a clustering similarity measure ranging from 0 (random) to 1 (perfect) to measure object segmentation. As in [2], we only use foreground pixels to compute ARI. Component VAEs in MONet use spatial broadcast decoders [43] that broadcast the latent representation to a full scale feature map before feeding them into the decoders, and the decoders therefore do not need upsampling. It has the implicit effect of encouraging the smoothness of the decoder outputs. To encourage similar behaviour, we add average pooling layers with stride 1 and kernel size 3 to our equivariant decoders. As shown in Table 1, using GAEs to model object components significantly improves reconstruction quality, which is consistent with our findings in single-object scenario. As shown in Table 2, using GAEs to model object components also leads to better object discovery in the low data regimes, but this advantage seems to diminish as the dataset becomes sufficiently large.

6 Conclusions, Limitations and Future Work

Conclusions We have proposed subsampling/upsampling operations that *exactly* preserve translation equivariance, and generalised them to define *exact* group equivariant subsampling/upsampling for discrete groups. We have used these layers in GAEs that allow learning low-dimensional representations that can be used to reliably manipulate pose and position of objects, and further showed how GAEs can be used to improve data efficiency in multi-object representation learning models.

Limitations and Future work Although the equivariance properties of subsampling layers also hold for Lie groups, we have not discussed the practical complexities that arise with the continuous case, where feature maps are only defined on a finite subset of the group rather than the whole group. We leave this as important future work, as well as application of equivariant subsampling for tasks other than representation learning where equivariance/invariance is desirable e.g. object classification, localization. Another limitation is that our work focuses on global equivariance, like most other works in the literature. An important direction is to extend to the case of local equivariances e.g. object-specific symmetries for multi-object scenes.

Acknowledgments and Disclosure of Funding

We would like to thank Adam R. Kosiosek for valuable discussion. We also thank Lewis Smith, Desi Ivanova, Sheheryar Zaidi, Neil Band, Fabian Fuchs, Ning Miao, and Matthew Willetts for providing feedback on earlier versions of the paper. JX gratefully acknowledges funding from Tencent AI Labs through the Oxford-Tencent Collaboration on Large Scale Machine Learning.

References

- [1] Bekkers, E. J. (2020). B-spline CNNs on Lie groups. In *ICLR*.
- [2] Burgess, C. P., Matthey, L., Watters, N., Kabra, R., Higgins, I., Botvinick, M., and Lerchner, A. (2019). Monet: Unsupervised scene decomposition and representation. *arXiv preprint arXiv:1901.11390*.
- [3] Chaman, A. and Dokmanić, I. (2020). Truly shift-invariant convolutional neural networks. *arXiv preprint arXiv:2011.14214*.
- [4] Chen, T. Q., Li, X., Grosse, R., and Duvenaud, D. (2018). Isolating sources of disentanglement in variational autoencoders. In *International Conference on Learning Representations*.
- [5] Cohen, T. and Welling, M. (2016). Group equivariant convolutional networks. In *International conference on machine learning*, pages 2990–2999.
- [6] Cohen, T. S., Geiger, M., Köhler, J., and Welling, M. (2018a). Spherical CNNs. In *ICLR*.
- [7] Cohen, T. S., Geiger, M., Köhler, J., and Welling, M. (2018b). Spherical CNNs. In *International Conference on Learning Representations*.
- [8] Cohen, T. S., Geiger, M., and Weiler, M. (2018c). Intertwiners between induced representations (with applications to the theory of equivariant neural networks). *arXiv preprint arXiv:1803.10743*.
- [9] Cohen, T. S., Geiger, M., and Weiler, M. (2019). A general theory of equivariant cnns on homogeneous spaces. *Advances in neural information processing systems*, 32:9145–9156.
- [10] Cohen, T. S. and Welling, M. (2017). Steerable cnns. In *International Conference on Learning Representations*.
- [11] Dieleman, S., De Fauw, J., and Kavukcuoglu, K. (2016). Exploiting cyclic symmetry in convolutional neural networks. In *International Conference on Machine Learning*, pages 1889–1898.
- [12] Dieleman, S., Willett, K. W., and Dambre, J. (2015). Rotation-invariant convolutional neural networks for galaxy morphology prediction. *Monthly notices of the royal astronomical society*, 450(2):1441–1459.
- [13] Engelcke, M., Kosiosek, A. R., Parker Jones, O., and Posner, I. (2020). GENESIS: Generative Scene Inference and Sampling of Object-Centric Latent Representations. *International Conference on Learning Representations (ICLR)*.
- [14] Esteves, C., Allen-Blanchette, C., Makadia, A., and Daniilidis, K. (2018). Learning SO(3) equivariant representations with spherical CNNs. In *ECCV*.
- [15] Esteves, C., Makadia, A., and Daniilidis, K. (2020). Spin-weighted spherical CNNs. In *NeurIPS*.
- [16] Finzi, M., Stanton, S., Izmailov, P., and Wilson, A. G. (2020). Generalizing convolutional neural networks for equivariance to Lie groups on arbitrary continuous data. In *ICML*.
- [17] Fuchs, F. B., Worrall, D. E., Fischer, V., and Welling, M. (2020). SE(3)-Transformers: 3D roto-translation equivariant attention networks. In *NeurIPS*.
- [18] Gens, R. and Domingos, P. M. (2014). Deep symmetry networks. *Advances in neural information processing systems*, 27:2537–2545.
- [19] Greff, K., Kaufman, R. L., Kabra, R., Watters, N., Burgess, C., Zoran, D., Matthey, L., Botvinick, M., and Lerchner, A. (2019). Multi-object representation learning with iterative variational inference. In *International Conference on Machine Learning*, pages 2424–2433. PMLR.

- [20] Harris, C. R., Millman, K. J., van der Walt, S. J., Gommers, R., Virtanen, P., Cournapeau, D., Wieser, E., Taylor, J., Berg, S., Smith, N. J., Kern, R., Picus, M., Hoyer, S., van Kerkwijk, M. H., Brett, M., Haldane, A., del Río, J. F., Wiebe, M., Peterson, P., Gérard-Marchant, P., Sheppard, K., Reddy, T., Weckesser, W., Abbasi, H., Gohlke, C., and Oliphant, T. E. (2020). Array programming with NumPy. *Nature*, 585(7825):357–362.
- [21] Higgins, I., Matthey, L., Pal, A., Burgess, C., Glorot, X., Botvinick, M., Mohamed, S., and Lerchner, A. (2017). beta-VAE: Learning basic visual concepts with a constrained variational framework. In *International Conference on Learning Representations*.
- [22] Hoogeboom, E., Peters, J. W., Cohen, T. S., and Welling, M. (2018). HexaConv. In *ICLR*.
- [23] Hunter, J. D. (2007). Matplotlib: A 2d graphics environment. *Computing in Science & Engineering*, 9(3):90–95.
- [24] Hutchinson, M., Le Lan, C., Zaidi, S., Dupont, E., Teh, Y. W., and Kim, H. (2021). Lietransformer: Equivariant self-attention for lie groups. In *Proceedings of the 38th International Conference on Machine Learning (ICML)*.
- [25] Johnson, J., Hariharan, B., Van Der Maaten, L., Fei-Fei, L., Lawrence Zitnick, C., and Girshick, R. (2017). Clevr: A diagnostic dataset for compositional language and elementary visual reasoning. In *Proceedings of the IEEE Conference on Computer Vision and Pattern Recognition*, pages 2901–2910.
- [26] Kabra, R., Burgess, C., Matthey, L., Kaufman, R. L., Greff, K., Reynolds, M., and Lerchner, A. (2019). Multi-object datasets. <https://github.com/deepmind/multi-object-datasets/>.
- [27] Kanazawa, A., Sharma, A., and Jacobs, D. (2014). Locally scale-invariant convolutional neural networks. *arXiv preprint arXiv:1412.5104*.
- [28] Kim, H. and Mnih, A. (2018). Disentangling by factorising. In *International Conference on Learning Representations*.
- [29] Kingma, D. P. and Ba, J. (2015). Adam: A method for stochastic optimization. In Bengio, Y. and LeCun, Y., editors, *3rd International Conference on Learning Representations, ICLR 2015, San Diego, CA, USA, May 7-9, 2015, Conference Track Proceedings*.
- [30] Kondor, R., Lin, Z., and Trivedi, S. (2018). Clebsch–Gordan nets: a fully Fourier space spherical convolutional neural network. In *NeurIPS*.
- [31] Locatello, F., Bauer, S., Lucic, M., Raetsch, G., Gelly, S., Schölkopf, B., and Bachem, O. (2019). Challenging common assumptions in the unsupervised learning of disentangled representations. In Chaudhuri, K. and Salakhutdinov, R., editors, *Proceedings of the 36th International Conference on Machine Learning*, volume 97 of *Proceedings of Machine Learning Research*, pages 4114–4124. PMLR.
- [32] Locatello, F., Weissenborn, D., Unterthiner, T., Mahendran, A., Heigold, G., Uszkoreit, J., Dosovitskiy, A., and Kipf, T. (2020). Object-centric learning with slot attention. *arXiv preprint arXiv:2006.15055*.
- [33] Marcos, D., Volpi, M., and Tuia, D. (2016). Learning rotation invariant convolutional filters for texture classification. In *2016 23rd International Conference on Pattern Recognition (ICPR)*, pages 2012–2017. IEEE.
- [34] Masci, J., Meier, U., Ciresan, D., and Schmidhuber, J. (2011). Stacked convolutional auto-encoders for hierarchical feature extraction. In *ICANN*.
- [35] Matthey, L., Higgins, I., Hassabis, D., and Lerchner, A. (2017). dsprites: Disentanglement testing sprites dataset. <https://github.com/deepmind/dsprites-dataset/>.
- [36] Paszke, A., Gross, S., Massa, F., Lerer, A., Bradbury, J., Chanan, G., Killeen, T., Lin, Z., Gimelshein, N., Antiga, L., Desmaison, A., Kopf, A., Yang, E., DeVito, Z., Raison, M., Tejani, A., Chilamkurthy, S., Steiner, B., Fang, L., Bai, J., and Chintala, S. (2019). Pytorch: An imperative style, high-performance deep learning library. In Wallach, H., Larochelle, H., Beygelzimer, A., d'Alché-Buc, F., Fox, E., and Garnett, R., editors, *Advances in Neural Information Processing Systems 32*, pages 8024–8035. Curran Associates, Inc.
- [37] Romero, D. W., Bekkers, E. J., Tomczak, J. M., and Hoogendoorn, M. (2020). Attentive group equivariant convolutional networks. In *ICML*.
- [38] Romero, D. W. and Hoogendoorn, M. (2020). Co-attentive equivariant neural networks: Focusing equivariance on transformations co-occurring in data. In *ICLR*.

- [39] Scherer, D., Müller, A., and Behnke, S. (2010). Evaluation of pooling operations in convolutional architectures for object recognition. In Diamantaras, K., Duch, W., and Iliadis, L. S., editors, *Artificial Neural Networks – ICANN 2010*, pages 92–101, Berlin, Heidelberg. Springer Berlin Heidelberg.
- [40] Simoncelli, E., Freeman, W., Adelson, E., and Heeger, D. (1992). Shiftable multiscale transforms. *IEEE Transactions on Information Theory*, 38(2):587–607.
- [41] Thomas, N., Smidt, T., Kearnes, S., Yang, L., Li, L., Kohlhoff, K., and Riley, P. (2018). Tensor field networks: Rotation-and translation-equivariant neural networks for 3d point clouds. *arXiv preprint arXiv:1802.08219*.
- [42] Waskom, M. L. (2021). seaborn: statistical data visualization. *Journal of Open Source Software*, 6(60):3021.
- [43] Watters, N., Matthey, L., Burgess, C. P., and Lerchner, A. (2019). Spatial broadcast decoder: A simple architecture for learning disentangled representations in vaes. *arXiv preprint arXiv:1901.07017*.
- [44] Weiler, M. and Cesa, G. (2019a). General e(2)-equivariant steerable cnns. In *Advances in Neural Information Processing Systems*, pages 14334–14345.
- [45] Weiler, M. and Cesa, G. (2019b). General E(2)-Equivariant Steerable CNNs. In *Conference on Neural Information Processing Systems (NeurIPS)*.
- [46] Weiler, M., Geiger, M., Welling, M., Boomsma, W., and Cohen, T. S. (2018a). 3d steerable cnns: Learning rotationally equivariant features in volumetric data. In *Advances in Neural Information Processing Systems*, pages 10381–10392.
- [47] Weiler, M., Hamprecht, F. A., and Storath, M. (2018b). Learning steerable filters for rotation equivariant cnns. In *Proceedings of the IEEE Conference on Computer Vision and Pattern Recognition*, pages 849–858.
- [48] Worrall, D. E., Garbin, S. J., Turmukhambetov, D., and Brostow, G. J. (2017). Harmonic networks: Deep translation and rotation equivariance. In *Proceedings of the IEEE Conference on Computer Vision and Pattern Recognition*, pages 5028–5037.
- [49] Xiao, H., Rasul, K., and Vollgraf, R. (2017). Fashion-mnist: a novel image dataset for benchmarking machine learning algorithms.
- [50] Yadan, O. (2019). Hydra - a framework for elegantly configuring complex applications. Github.
- [51] Zhang, R. (2019). Making convolutional networks shift-invariant again. In *International Conference on Machine Learning*, pages 7324–7334.
- [52] Zhao, S., Song, J., and Ermon, S. (2017). Infovae: Information maximizing variational autoencoders. *arXiv preprint arXiv:1706.02262*.

A Preliminaries

A.1 Group, Coset and Quotient Space

A *group* G is a set of elements equipped with a binary operation (denoted as \cdot) that satisfies the following group axioms:

1. (Closure) For all $a, b \in G$, $a \cdot b \in G$.
2. (Associative) For all $a, b, c \in G$, $(a \cdot b) \cdot c = a \cdot (b \cdot c)$.
3. (Identity element) There exists an identity element e in G such that, for any $a \in G$ we have $e \cdot a = a \cdot e = a$.
4. (Inverse element) For each $a \in G$, there exists an element $b \in G$ such that $a \cdot b = b \cdot a = e$ where e is the identity element.

The centered dot \cdot can sometimes be omitted if there is no ambiguity.

In this work, we are mainly interested in symmetry groups where each group element is associated with a symmetry of a pattern, which is a transformation that leaves the pattern invariant. In symmetry groups, the binary operation corresponds to composition of transformations.

A subset H contained within G is a *subgroup* of G if it forms a group on its own under the same binary operation. Given a subgroup H and an arbitrary group element $g \in G$, one can define *left cosets* of H as follows:

$$gH = \{g \cdot h \mid h \in H\}$$

The left cosets of H form a partition of G for any choice of H , i.e. the union of all cosets is G and all cosets defined above are either identical or have empty interception. The set of all left cosets is called the *quotient space* and is denoted as $G/H = \{gH \mid g \in G\}$.

As an example, all integers \mathbb{Z} under addition forms a group and all multiples of n , denoted as $n\mathbb{Z}$ is a subgroup of \mathbb{Z} . For any integer $k \in \mathbb{Z}$, the set $n\mathbb{Z} + k$ containing all integers that has the remainder as k divided by n , is a coset of $n\mathbb{Z}$. There are n distinct cosets like this, and they form the quotient space $\mathbb{Z}/n\mathbb{Z}$.

A.2 Group Homomorphism, Group Actions and Group Equivariance

Given two groups (G, \cdot_G) and (H, \cdot_H) , a *group homomorphism* from G to H is function $f : G \rightarrow H$ such that for any $u, v \in G$

$$f(u \cdot_G v) = f(u) \cdot_H f(v).$$

It is a special mapping between two groups that is compatible with group structures. If f is an one-to-one mapping, we call it a *group isomorphism*. Two groups G_1 and G_2 are isomorphic if there is an isomorphism between them, and this is written as $G_1 \cong G_2$.

A *group action* is a group homomorphism from a given group G to the group of transformations on a space \mathbf{X} . We say the group G acts on the space \mathbf{X} and the transformation corresponding to $g \in G$ is a bijection on \mathbf{X} that maps x to $g \cdot x$.

If the group actions of G on spaces \mathbf{X} and \mathbf{Y} are both defined, a function $f : \mathbf{X} \rightarrow \mathbf{Y}$ is said to be *group equivariant* if

$$g \cdot f(x) = f(g \cdot x)$$

A.3 Homogeneous Spaces and Lifting Feature Maps

If the action of a group G on the space \mathbf{X} is defined, and the action is transitive (i.e. $\forall x, x' \in \mathbf{X}, \exists g \in G$, s.t. $x' = g \cdot x$), we refer to \mathbf{X} as being a homogeneous space for G . There is a natural one-to-one correspondence between the homogeneous space \mathbf{X} and disjoint subsets of the group G . Given an arbitrary origin $x_0 \in \mathbf{X}$, $H = \{g \in G \mid g \cdot x_0 = x_0\}$ is a subgroup of G , where H is called the stabiliser of the origin. Because the group action on \mathbf{X} is transitive, every element $x \in \mathbf{X}$ corresponds to a left coset in $s(x; x_0)H \in G/H$, where $s(x; x_0)$ is (any) group element that transforms x_0 to x . It can be shown that for $x, x' \in \mathbf{X}, x \neq x', s(x; x_0)$ and $s(x'; x_0)$ are disjoint.

Because spatial data is often represented as functions on the homogeneous space $f_{\mathbf{X}} : x_i \mapsto f_i$, while lifting-based group equivariant neural networks operate on feature maps defined on the group, there is usually an operation called *lifting*, that maps the data to the feature space of functions on the group, before applying equivariant modules. Using the correspondence between \mathbf{X} and the quotient space G/H , we can map each pair (x_i, f_i) to the set $\{(g, f_i) | g \in s(x_i; x_0)H\}$. It can be seen as lifting the input feature map $f_{\mathbf{X}} : x_i \mapsto f_i$ to the feature map $\text{LIFT}(f_{\mathbf{X}}) : g \mapsto f_i$ for $g \in s(x_i; x_0)H$. In this work, we assume all input feature maps have been lifted to feature maps on the group.

A.4 Wallpaper Groups

Wallpaper groups categorise symmetries of repetitive patterns on a 2D plane. For simplicity, we only considered 3 different types of wallpaper symmetry groups $p1$, $p4$, and $p4m$ in this work following [5]. These groups are named using the crystallographic notation, where p stands for primitive cells, the next digit indicates the highest order of rotational symmetries, and m stands for mirror reflection. All symmetries contained in these groups can be deduced from their name:

- $p1$: All 2D integer translations.
- $p4$: All compositions of 2D integer translations and rotations by a multiple of 90 degrees.
- $p4m$: All compositions of elements in $p4$ and the mirror reflection.

All three groups $p1$, $p4$, and $p4m$ can be constructed from basic additive groups of integers \mathbb{Z} and cyclic groups C_n using the inner semi-direct product. Given a group G with a normal subgroup N (i.e. $\forall n \in N, g \in G, gng^{-1} \in N$), a subgroup H (not necessarily a normal subgroup), if G is the product of subgroups $G = NH = \{nh | n \in N, h \in H\}$, and $N \cap H = \{e\}$, we say G is a inner semi-direct product of N and H , written as $G = N \rtimes H$. Using semi-direct product, $p1$, $p4$, and $p4m$ can be expressed as:

$$\begin{aligned} p1 &\cong \mathbb{Z}^2 \\ p4 &\cong \mathbb{Z}^2 \rtimes C_4 \\ p4m &\cong \mathbb{Z}^2 \rtimes (C_4 \rtimes C_2) \end{aligned} \quad (11)$$

If $G \cong N \rtimes H$, the binary and inverse operations for G can be determined from its subgroups N and H . We represent group elements in G as a tuple (n, h) where $n \in N$ and $h \in H$. Let $\phi_h(n) = hnh^{-1}$, the binary operation on G can be given by:

$$(n_1, h_1) \cdot (n_2, h_2) = (n_1 \phi_{h_1}(n_2), h_1 h_2)$$

and the inverse for element in G can also be derived from the above:

$$(n, h)^{-1} = (\phi_{h^{-1}}(n^{-1}), h^{-1})$$

These properties can be used to simplify the implementation of the considered groups $p1$, $p4$, and $p4m$ following the decomposition in Equation (11), and the operations for basic groups \mathbb{Z} and C_n are easy to implement.

A.5 Feature Maps in G-CNNs

A general mathematical framework is introduced in [9] to specify convolutional feature spaces used in G-CNNs, and feature maps are treated as fields over a homogeneous space. It covers most previous works on equivariant neural networks including [5, 7, 10, 44]. Under this framework, one way to represent fields is through constrained functions defined on the whole symmetry group, also known as Mackey functions [9].

Formally, let G be a symmetry group, and $H \leq G$ together with G determines the homogeneous space G/H . For a group representation (ρ, V) of H , the action of the whole group G on fields can be described by an induced representation $\pi = \text{Ind}_H^G \rho$, whose realisation depends on how we represent these fields. Below we specify the feature space \mathcal{I}_M ⁴ for the Mackey function field representation discussed in [8, 9]:

$$\mathcal{I}_M = \{f : G \rightarrow V | f(gh) = \rho(h^{-1})f(g), \forall g \in G, h \in H\} \quad (12)$$

⁴ \mathcal{I}_M corresponds to \mathcal{I}_G in [9]

which forms a vector space. Moreover, when ρ is a *regular representation*, which is the implicit choice of [5, 11, 12, 18, 27, 33], fields can also be represented as unconstrained functions on G and the feature space can be written as

$$\mathcal{I}_G = \{f : G \rightarrow V'\}$$

with V' being a different vector space from V . If ρ is a regular representation.

Feature maps are represented as functions on G in both \mathcal{I}_M and \mathcal{I}_G , even though \mathcal{I}_M have additional conditions given in Equation (12). Moreover, the induced representation $\pi = \text{Ind}_H^G \rho$ for them have the same form:

$$[\pi(u)f](g) = f(u^{-1}g)$$

B Equivariant Subsampling and Upsampling

B.1 Constructing Φ

In Section 2.3, we provide a simple construction of the equivariant map $\Phi : \mathcal{I}_G \rightarrow G/K$ which gives the sampling indexes. The construction is a valid one if the argmax is unique. In practice one can insert arbitrary equivariant layers to f before and after we take the norm $\|\cdot\|_1$ to avoid a non-unique argmax (see Appendix E). However, in theory, there could be cases that the argmax is always non-unique. We discuss this case below and provide a more complex construction for it.

One cannot avoid a non-unique argmax in Equation (7) when the input feature map $f \in \mathcal{I}_G$ has inherent symmetries, i.e. there exists $u \in G, u \neq e$, such that $f = \pi(u)f$. Assuming there is a unique argmax g^* such that $g^* = \arg \max_{g \in G} \|f(g)\|_1$, we would have:

$$f(u \cdot g^*) = f(g^*) = \max_{g \in G} \|f(g)\|_1$$

Therefore $u \cdot g^*$ is also a valid argmax, hence the argmax is not unique. For example, when f is a feature map representing a center-aligned circle, we would have $f = \pi(u)f$, where $u \in O(2)$ is associated with an arbitrary rotation around the center. One cannot find a unique argmax g^* for this example, because the feature map would take the same function values at $u \cdot g^*$.

Under the circumstance described above, the argmax operation would return a set of elements where each one attains the function's largest values. We denote it as $S^* = \arg \max_{g \in G} \|f(g)\|_1$, where S^* is a subset of G . To obtain the sampling index (a coset) pK , we sample uniformly from the set S^* , and let Φ outputs pK where $p \sim S^*$. In this case, the map Φ is still equivariant in distribution even though it is now a stochastic map.

Note that it is possible to consider more sophisticated solutions or even use learnable modules for Φ , which we leave for future work.

B.2 Multiple Subsampling Layers

Translation equivariant subsampling We can stack convolutional and translation equivariant subsampling layers to construct exactly translation equivariant CNNs. Unlike standard CNNs, each translation equivariant subsampling layer with a scale factor c_k outputs a subsampling index i_k in addition to the feature maps. Hence the equivariant representation output by the CNN with L subsampling layers is a final feature map f_L and a L -tuple of sampling indices (i_1, \dots, i_L) .

In the multi-layer case, the l -th subsampling layer takes in a feature map f on $\prod_{k=1}^{l-1} c_k \mathbb{Z}$ and outputs: 1) a feature map on $\prod_{k=1}^l c_k \mathbb{Z}$ and 2) a subsampling index $i_l \in \prod_{k=1}^{l-1} c_k \mathbb{Z} / \prod_{k=1}^l c_k \mathbb{Z} \cong \mathbb{Z} / c_l \mathbb{Z}$ given by:

$$\left(\prod_{k=1}^{l-1} c_k \right) \cdot i_l = p_l = \Phi_c(f) = \text{mod}(\arg \max_{x \in (\prod_{k=1}^{l-1} c_k) \mathbb{Z}} \|f(x)\|_1, \prod_{k=1}^l c_k)$$

This is equivalent to treating the input feature map f as a feature map f' defined on \mathbb{Z} (i.e. mapping the support of f from $\prod_{k=1}^{l-1} c_k \mathbb{Z}$ to \mathbb{Z} via division by $\prod_{k=1}^{l-1} c_k$), and the subsampling layer outputting: 1) a feature map on $c_l \mathbb{Z}$ and 2) a subsampling index $i_l \in \mathbb{Z} / c_l \mathbb{Z}$ given by:

$$i_l = \text{mod}(\arg \max_{x \in \mathbb{Z}} \|f'(x)\|_1, c_l)$$

Hence the tuple (i_1, \dots, i_L) that contains the sampling indices of all layers can be expressed equivalently as a single integer:

$$r_{\text{eq}} = \sum_{l=1}^L p_l = \sum_{l=1}^L \left(\prod_{k=1}^{l-1} c_k \right) \cdot i_l$$

where $r_{\text{eq}} \in \mathbb{Z} / \left(\prod_{k=1}^L c_k \right) \mathbb{Z}$. Note that the conversion between r_{eq} and (i_1, \dots, i_L) can be seen as the conversion between *mixed radix notation* and decimal notation. Mixed radix notation is a mixed base numeral system where the numerical base varies from position to position, as opposed to base- n systems that have the same base for all positions⁵. Thus there is an one-to-one correspondence between the two. Moreover, when the input feature map is translated to the right by $t \in \mathbb{Z}$, r_{eq} would become $\text{mod}(r_{\text{eq}} + t, \prod_{k=1}^L c_k)$. See the statement of this result for the general group case in Proposition B.1 and its proof in Appendix D.3.

Group equivariant subsampling Similarly, given an input feature map $f \in \mathcal{I}_G$, we can construct CNNs/G-CNNs with multiple equivariant subsampling layers by specifying a sequence of nested subgroups $G = G_0 \geq G_1 \geq \dots \geq G_L$. The l -th subsampling layer takes in a feature map on G_{l-1} , outputs a feature map on G_l and a sampling index $p_l G_l \in G_{l-1}/G_l$. Formally, the l -th subsampling layer can be written as:

$$S_b \downarrow_{G_l}^{G_{l-1}} : \mathcal{I}_{G_{l-1}} \rightarrow \mathcal{I}_{G_l} \times G_{l-1}/G_l$$

The equivariant representation output by the CNNs/G-CNNs with L subsampling layers is a feature map in $f_L \in G_L$ and a L -tuple $(p_1 G_1, p_2 G_2, \dots, p_L G_L)$.

Similar to the 1D translation case, the sampling index tuple $(p_1 G_1, p_2 G_2, \dots, p_L G_L)$ can be expressed equivalently as a single element in the quotient space G/G_L :

$$r_{\text{eq}} = (\bar{p}_1 \bar{p}_2 \dots \bar{p}_L) G_L = \nu(p_1 G_1, p_2 G_2, \dots, p_L G_L) \quad (13)$$

where \bar{p}_l denote the coset representative for the quotient space G_{l-1}/G_l . ν is a bijection from r_{eq} to the tuple, whose inverse can be computed by the following recursive procedure:

$$\begin{aligned} p'_1 G_L &= r_{\text{eq}} \\ p'_l &= \bar{p}'_{l-1} \cdot p'_{l-1} \\ (p'_1 G_1, p'_2 G_2, \dots, p'_L G_L) &= \nu^{-1}(r_{\text{eq}}) \end{aligned} \quad (14)$$

Proposition B.1. ν^{-1} is the inverse of ν , hence ν is bijective. And $\forall u \in G$ we have:

$$u \cdot \nu(p_1 G_1, p_2 G_2, \dots, p_L G_L) = \nu(u \cdot (p_1 G_1, p_2 G_2, \dots, p_L G_L)).$$

C Group Equivariant Autoencoders

In Appendix B.2 we discussed that we can stack multiple subsampling layers by specifying a sequence of nested groups $G = G_0 \geq G_1 \geq \dots \geq G_L$, and the CNN/G-CNNs with L subsampling layers would produce a feature map on G_L and a tuple $z_{\text{eq}} = (p_1 G_1, p_2 G_2, \dots, p_L G_L)$. Furthermore, we know from Proposition B.1 that there is an one-to-one correspondence between the tuple representation z_{eq} and the single group element representation $r_{\text{eq}} = \nu(z_{\text{eq}}) \in G/G_L$. For group equivariant autoencoders, we specify a sequence of subgroups but with $G_L = \{e\}$. In this case, r_{eq} would simply become a group element in G . And the group action simplifies to left-multiplying the corresponding group elements.

Although one can simply use the tuple output by the encoder to perform upsampling in the decoder (and hence use the same sequence of nested subgroups), this is not strictly necessary as one can use a different sequence of nested subgroups for the decoder and obtain the tuple using the decomposition procedure in Equation (14). Moreover, for more efficient implementation of GAEs, one does not need to pass through Φ in Equation (7) for every subsampling layer. It would suffice to obtain the tuple of subsampling indexes from the first subsampling layer using:

$$(p_1 G_1, p_2 G_2, \dots, p_L G_L) = \nu^{-1}(\arg \max_{g \in G} \|f(g)\|_1) \quad (15)$$

⁵A commonly used example of mixed radix notation is to express time, where e.g. 12:34:56 has a base of 24 for the hour digit, base 60 for the minute digit and base 60 for the second digit.

D Proofs

D.1 Proof of Lemma 2.1 (See page 5)

Lemma 2.1. π' defines a valid group action of G on the space $\mathcal{I}_K \times G/K$.

Proof. Since \bar{p} and \overline{up} are coset representatives for pK and $(up)K$, we can let $p = \bar{p}k_p$, $up = \overline{up}k_{up}$, where $k_p, k_{up} \in K$. From Equation (6), note that $\bar{p}' = \overline{up} = upk_{up}^{-1}$. Hence

$$\begin{aligned} \bar{p}'^{-1}u\bar{p} &= (upk_{up}^{-1})^{-1}u(pk_p^{-1}) \\ &= k_{up}p^{-1}u^{-1}upk_p^{-1} \\ &= k_{up}k_p^{-1} \in K \end{aligned} \tag{16}$$

Hence $\pi'(u)$ (as defined in Equation (6)) defines a transformation from the space $\mathcal{I}_K \times G/K$ to itself.

To prove π' is a group action, we would like to show that for all $u, u' \in G$

$$\pi'(u')(\pi'(u)[f_b, pK]) = \pi'(u'u)[f_b, pK]$$

Let $[f'_b, p'K] = \pi'(u)[f_b, pK]$ and $[f''_b, p''K] = \pi'(u')[f_b, pK]$, by the definition of π' in Equation (6), we have

$$p''K = ((u'u)p)K = u'(upK) = u'(p'K)$$

and

$$f''_b = \pi(\bar{p}''^{-1}(u'u)\bar{p})f_b = \pi(\bar{p}''^{-1}u'\bar{p}')\pi(\bar{p}'^{-1}u\bar{p})f_b = \pi(\bar{p}''^{-1}u'\bar{p}')f'_b.$$

Hence

$$[f''_b, p''K] = \pi'(u')[f'_b, p'K]$$

It is easy to also check that

$$[f_b, pK] = \pi'(e)[f_b, pK]$$

Therefore π' defines a valid group action. \square

D.2 Proof of Proposition 2.2 (See page 5)

Proposition 2.2. *If the action of group G on the space \mathcal{I}_G and $\mathcal{I}_K \times G/K$ are specified by π, π' (as defined in Equations (3) and (6)), and $\Phi : \mathcal{I}_G \rightarrow G/K$ is an equivariant map, then the operations $S_b \downarrow_K^G$ and $S_u \uparrow_K^G$ as defined in Equations (4) and (5) are equivariant maps between \mathcal{I}_G and $\mathcal{I}_K \times G/K$.*

Proof. We first define a *restrict* operation on $f \in \mathcal{I}_G$ and an *extend* operation on $f_1 \in \mathcal{I}_K$:

$$\begin{aligned} f \downarrow_K^G(k) &= f(k), \quad k \in K \\ f_1 \uparrow_K^G(g) &= \begin{cases} f_1(g) & g \in K \\ \mathbf{0} & g \notin K \end{cases} \end{aligned}$$

where $f \downarrow_K^G \in \mathcal{I}_K$ and $f_1 \uparrow_K^G \in \mathcal{I}_G$.

Recall that $s : G/K \rightarrow G$ is a function choosing a coset representative \bar{p} for each coset pK . Using the restrict operation, the subsampling operation $S_b \downarrow_K^G(f; \Phi)$ in Equation (4) can equivalently be described as:

$$\begin{aligned} pK &= \Phi(f) \\ f_b &= [\pi(\bar{p}^{-1})f] \downarrow_K^G \\ [f_b, pK] &= S_b \downarrow_K^G(f; \Phi) \end{aligned}$$

And the upsampling operation $S_u \uparrow_K^G$ can be rewritten using the extend operation as:

$$f_u = S_u \uparrow_K^G(f_1, pK) = \pi(\bar{p})(f_1 \uparrow_K^G)$$

For any $u \in G$ let $f' = \pi(u)f$ and $[f'_b, p'K] = \pi'(u)[f_b, pK]$ where π and π' are specified in Equation (3) and Equation (6) respectively. Since Φ is equivariant, we have

$$\Phi(f') = \Phi(\pi(u)f) = u \cdot \Phi(f) = u \cdot pK = p'K \quad (17)$$

Recall that $\bar{p}'^{-1}u\bar{p} = k_{up}k_p^{-1}$ from Equation (16). Hence $\bar{p}'^{-1} = k_{up}k_p^{-1}\bar{p}^{-1}u^{-1}$ and we have

$$\begin{aligned} [\pi(\bar{p}'^{-1})f'] \downarrow_K^G &= [\pi(k_{up}k_p^{-1}\bar{p}^{-1}u^{-1})f'] \downarrow_K^G \\ &= \pi(k_{up}k_p^{-1})[\pi(\bar{p}^{-1})\pi(u^{-1})f'] \downarrow_K^G \\ &= \pi(k_{up}k_p^{-1})[\pi(\bar{p}^{-1})f] \downarrow_K^G \\ &= \pi(k_{up}k_p^{-1})f_b = f'_b \end{aligned} \quad (18)$$

From Equations (17) and (18), $S_b \downarrow_K^G$ is equivariant, i.e.

$$\pi'(u)S_b \downarrow_K^G(f; \Phi) = S_b \downarrow_K^G(\pi(u)f; \Phi)$$

For the upsampling operation, let $[f'_1, p'_1K] = \pi'(u)[f_1, p_1K]$ and $f'_u = \pi(u)f_u$. From Equation (6) we have $f'_1 = \pi(\bar{p}'^{-1}u\bar{p})f_1$. Hence

$$\begin{aligned} S_u \uparrow_K^G(f'_1, p'_1K) &= \pi(\bar{p}')f'_1 \uparrow_H^G \\ &= \pi(\bar{p}')[\pi(\bar{p}'^{-1}u\bar{p})f_1] \uparrow_H^G \\ &= \pi(\bar{p}')\pi(\bar{p}'^{-1}u\bar{p})(f_1 \uparrow_H^G) \\ &= \pi(u\bar{p})f_1 \uparrow_H^G = \pi(u)f_u = f'_u \end{aligned}$$

Therefore, $S_u \uparrow_K^G$ is equivariant, i.e.

$$\pi(u)S_u \uparrow_K^G([f_1, p_1K]) = S_u \uparrow_K^G(\pi'(u)[f_1, p_1K])$$

□

D.3 Proof of Proposition B.1 (See page 16)

Proposition B.1. ν^{-1} is the inverse of ν , hence ν is bijective. And $\forall u \in G$ we have:

$$u \cdot \nu(p_1G_1, p_2G_2, \dots, p_LG_L) = \nu(u \cdot (p_1G_1, p_2G_2, \dots, p_LG_L)).$$

Proof. Firstly, we prove that $\nu^{-1} \circ \nu$ is an identity map, i.e. $\nu^{-1} \circ \nu = \mathbb{1}_z$. Let $r_{\text{eq}} = \nu(p_1G_1, p_2G_2, \dots, p_LG_L) = (\bar{p}_1\bar{p}_2 \dots \bar{p}_L)G_L$ and $(p'_1G_1, p'_2G_2, \dots, p'_LG_L) = \nu^{-1}(r_{\text{eq}})$. From Equation (14), we know that $p'_1G_L = r_{\text{eq}}$. Hence we can let $p'_1 = \bar{p}_1\bar{p}_2 \dots \bar{p}_LG_L$ where $g_L \in G_L$. Since $(\bar{p}_2\bar{p}_3 \dots \bar{p}_L) \in G_1$, for $l = 1$ we have

$$\begin{aligned} \bar{p}'_1 &= \bar{p}_1 \\ p'_2 &= \bar{p}'_1^{-1} \cdot p'_1 = \bar{p}_2\bar{p}_3 \dots \bar{p}_LG_L \end{aligned}$$

And recursively, for $l = 1, \dots, L$ we would have

$$\begin{aligned} \bar{p}'_l &= \bar{p}_l \\ p'_{l+1} &= \bar{p}'_{l+1} \dots \bar{p}_LG_L \end{aligned}$$

Hence $(p_1G_1, p_2G_2, \dots, p_LG_L) = (p'_1G_1, p'_2G_2, \dots, p'_LG_L)$ and $\nu^{-1} \circ \nu = \mathbb{1}_z$.

Secondly, we prove that $\nu \circ \nu^{-1}$ is also an identity map, i.e. $\nu \circ \nu^{-1} = \mathbb{1}_r$. Let $(p'_1G_1, p'_2G_2, \dots, p'_LG_L) = \nu^{-1}(r_{\text{eq}})$ and $r'_{\text{eq}} = \nu(p'_1G_1, p'_2G_2, \dots, p'_LG_L)$. From Equation (14), we have $r_{\text{eq}} = p'_1G_L$ and $p'_l = \bar{p}'_{l-1} \cdot p_{l-1}$. Hence

$$r_{\text{eq}} = p'_1G_L = \bar{p}'_1 p'_2G_L = \dots = \bar{p}'_1 \bar{p}'_2 \dots \bar{p}'_{L-1} p'_L G_L = \bar{p}'_1 \bar{p}'_2 \dots \bar{p}'_L G_L = r'_{\text{eq}}$$

Therefore $\nu \circ \nu^{-1} = \mathbb{1}_r$ and ν is bijective.

Lastly, we prove ν is equivariant. Let $(p'_1 G_1, p'_2 G_2, \dots, p'_L G_L) = u \cdot (p_1 G_1, p_2 G_2, \dots, p_L G_L)$ where the group action is implied by Equation (6). From Equation (16), we know that when $u \in G$, $\pi(\bar{p}'_1{}^{-1} u \bar{p}_1) \in G_1$. Recursively, we have

$$\bar{p}'_l{}^{-1} \dots \bar{p}'_2{}^{-1} \bar{p}'_1{}^{-1} u \bar{p}_1 \bar{p}_2 \dots \bar{p}_l \in G_l \quad (19)$$

for $l = 1, \dots, L$. When $l = L$, from $\bar{p}'_L{}^{-1} \dots \bar{p}'_2{}^{-1} \bar{p}'_1{}^{-1} u \bar{p}_1 \bar{p}_2 \dots \bar{p}_L \in G_L$, we have

$$\bar{p}'_1 \bar{p}'_2 \dots \bar{p}'_L G_L = u \cdot (\bar{p}_1 \bar{p}_2 \dots \bar{p}_L G_L)$$

Hence $u \cdot \nu(p_1 G_1, p_2 G_2, \dots, p_L G_L) = \nu(u \cdot (p_1 G_1, p_2 G_2, \dots, p_L G_L))$. So that the group action given by Equation (6) is simplified to the left-action on the single group element. \square

D.4 Proof of Proposition 3.1 (See page 6)

Proposition 3.1. *When ENC and DEC are given by Equations (8) and (9), and the group actions are specified as in Equation (3) and Equation (6), for any $g \in G$ and $f \in \mathcal{I}_G$, we have*

$$\begin{aligned} [z_{\text{inv}}, g \cdot z_{\text{eq}}] &= \text{ENC}(\pi(g)f) \\ \pi(g)\hat{f} &= \text{DEC}(z_{\text{inv}}, g \cdot z_{\text{eq}}) \end{aligned}$$

Proof. Let $f, f' \in \mathcal{I}_G$ be the input feature maps where $f' = \pi(g)f$. Let $[f_l, p_l G_l]$ and $[f'_l, p'_l G_l]$ be the feature maps and subsampling indexes output by the l -th subsampling layer for f and f' respectively. Let $[z_{\text{inv}}, z_{\text{eq}}] = \text{ENC}(f)$ and $[z'_{\text{inv}}, z'_{\text{eq}}] = \text{ENC}(f')$ and let $r_{\text{eq}} = \nu(z_{\text{eq}})$, $r'_{\text{eq}} = \nu(z'_{\text{eq}})$ where ν is given in Equation (13).

From Equation (6) and the equivariance of $G\text{-CNN}_l(\cdot)$, we have

$$f'_1 = \pi(\bar{p}'_1{}^{-1} g \bar{p}_1) f_1$$

and recursively:

$$f'_l = \pi((\bar{p}'_1 \bar{p}'_2 \dots \bar{p}'_l)^{-1} g (\bar{p}_1 \bar{p}_2 \dots \bar{p}_l)) f_l \quad (20)$$

where $l = 1, \dots, L$ and $(\bar{p}'_1 \bar{p}'_2 \dots \bar{p}'_l)^{-1} g (\bar{p}_1 \bar{p}_2 \dots \bar{p}_l) \in G_l$ (see Equation (19)).

Since $G_L = \{e\}$ when $l = L$, we have

$$(\bar{p}'_1 \bar{p}'_2 \dots \bar{p}'_L)^{-1} g (\bar{p}_1 \bar{p}_2 \dots \bar{p}_L) = e$$

Hence

$$\begin{aligned} f'(e) &= f(e) \\ (\bar{p}'_1 \bar{p}'_2 \dots \bar{p}'_L) &= g \cdot (\bar{p}_1 \bar{p}_2 \dots \bar{p}_L) \end{aligned}$$

which can be rewritten as

$$\begin{aligned} z'_{\text{inv}} &= z_{\text{inv}} \\ r'_{\text{eq}} &= g \cdot r_{\text{eq}} \end{aligned}$$

From Proposition B.1 we have

$$z'_{\text{eq}} = \nu^{-1}(r'_{\text{eq}}) = \nu^{-1}(g r_{\text{eq}}) = g \cdot \nu^{-1}(r_{\text{eq}}) = g \cdot z_{\text{eq}}$$

Therefore, for the encoders we have $[z_{\text{inv}}, g \cdot z_{\text{eq}}] = \text{ENC}(\pi(g)f)$.

For the decoders, let

$$z'_{\text{eq}} = (p'_1 G_1, p'_2 G_2, \dots, p'_L G_L) = g \cdot z_{\text{eq}}$$

Since the feature map at the l -th subsampling layer is transformed according to Equation (20), the sampling index is transformed accordingly:

$$p'_l G_l = (\bar{p}'_{l-1}{}^{-1} \dots \bar{p}'_2{}^{-1} \bar{p}'_1{}^{-1} g \bar{p}_1 \bar{p}_2 \dots \bar{p}_{l-1}) p_l G_L$$

From the definition of equivariant upsampling in Equation (5), we have

$$f'_{l-1} = \pi(\bar{p}'_{l-1}{}^{-1} \dots \bar{p}'_2{}^{-1} \bar{p}'_1{}^{-1} g \bar{p}_1 \bar{p}_2 \dots \bar{p}_{l-1}) f_{l-1}$$

where $l = L, \dots, 1$. When $l = 1$, we have $f'_0 = \pi(g)f_0$ so that $\pi(g)\hat{f} = \text{DEC}(z_{\text{inv}}, g \cdot z_{\text{eq}})$. \square

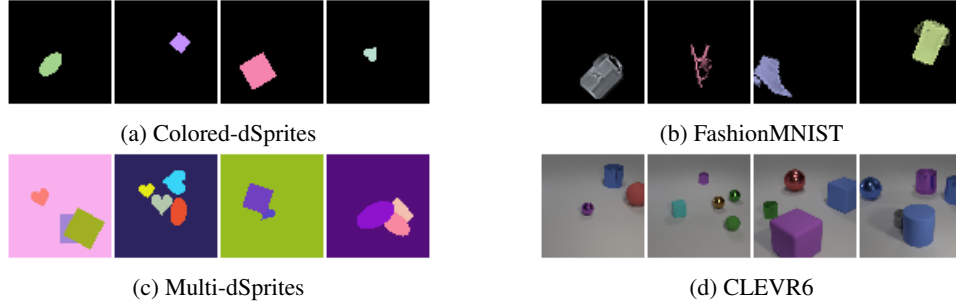


Figure 6

E Implementation Details

In this section, we outline a few important implementation details, and leave other details to the reference code at <https://github.com/jinxu06/gsubsampling>.

E.1 Data

For Colored-dSprites and FashionMNIST datasets, we add colours to grayscale images from [35] and [49] by sampling random scaling for each channel uniformly between 0.5 and 1 following [31]. For FashionMNIST, we also apply zero-paddings to images to reach the size of 64×64 . We then translate the images with random displacements uniformly sampled from $\{(x, y) | -18 \leq x, y \leq 18, x, y \in \mathbb{Z}\}$, and rotate the images with uniformly sampled degrees from $\{\frac{360 \times k}{32} | k = 0, \dots, 32\}$. We use the original Multi-dSprites dataset as provided in [26]. For CLEVR6, we crop images from the original CLEVR [25] at y-coordinates (29, 221) bottom and top, and at x-coordinates (64, 256) left and right as stated in [2]. We then resize the images to 64×64 so that we can use the same model for both multi-object datasets. We only use images with up to 6 objects in CLEVR following [19]. For evaluation, we use a randomly sampled test set with 10000 examples that has no overlap with training data for all datasets. In Figure 6, we show examples from different datasets.

E.2 Model Architectures

The equivariant map Φ One can insert arbitrary equivariant layers before and after we take the norm $\|\cdot\|_1$ in Equation (7). In experiments, we apply mean subtraction followed by average pooling with kernel size 5 before taking the norm, and apply Gaussian blur with kernel size 15 after taking the norm. They are inserted in the purpose of smoothing feature maps and avoiding non-unique argmax when possible (in Appendix B.1 we discuss the case when non-unique argmax cannot be avoided). In practice, we use Equation (15) to obtain all subsampling indexes at the same time rather than passing through Φ multiple times.

Autoencoders For all single object experiments, we use 5 layers of (G -)equivariant convolutional layers in encoders, and the decoders mirror the architecture of the encoders except for the output layers. In baseline models, we use strided convolution as a way to perform subsampling/upsampling, while in equivariant models we use equivariant downsampling/upsampling. We rescale the number of channels such that the total number of parameters of the models roughly match one another. However, exact correspondence is not achievable because exact equivariant models use equivariant subsampling to transform feature maps into vectors at the final layer of the encoder, while baseline models apply flattening. Please see the reference implementation for other details about network architectures.

We use scale factor 2 for all subsampling and upsampling layers in baseline models. For GAE- $p1$, the feature maps at each layer are defined on the following chain of nested subgroups: $\mathbb{Z}^2 \geq (2\mathbb{Z})^2 \geq (4\mathbb{Z})^2 \geq (8\mathbb{Z})^2 \geq (16\mathbb{Z})^2 \geq \{e\}$. For GAE- $p4$, we use $\mathbb{Z}^2 \times C_4 \geq (2\mathbb{Z})^2 \times C_4 \geq (4\mathbb{Z})^2 \times C_4 \geq (8\mathbb{Z})^2 \times C_4 \geq (16\mathbb{Z})^2 \times C_2 \geq \{e\}$. And for GAE- $p4m$, we use $\mathbb{Z}^2 \times (C_4 \times C_2) \geq (2\mathbb{Z})^2 \times (C_4 \times C_2) \geq (4\mathbb{Z})^2 \times (C_4 \times C_2) \geq (8\mathbb{Z})^2 \times (C_4 \times C_2) \geq (16\mathbb{Z})^2 \times (C_2 \times C_2) \geq \{e\}$.

Object discovery For baseline models, we adopt the exact same architecture as the original MONet [2] using the implementation provided by [13]. For MONet-GAEs, we simply replace Component VAEs in the original MONet with our V-GAEs. Both Component VAEs and V-GAEs have a latent size of 16.

E.3 Hyperparameters

For all single object experiments, we use Adam optimizer [29] with a learning rate of 0.0001 and a batch size of 16. We use 16-bits precision to enable faster training and reduce memory consumption. For experiments on multi-object datasets, hyperparameters will match the original MONet [2] except that we still use a batch size of 16 instead of 64 stated in the original paper. This is because we observed that in the low data regime, batch size 16 trains faster and performs no worse than batch size 64 for the problems we considered here.

E.4 Computational Resources

In theory, the only computational overhead is caused by computing sampling indices, which is negligible compared to the forward pass of (G -)Convolutional layers. In practice, our current implementation uses `torch.gather` to perform subsampling, and relies on for-loops over data batches when applying group actions to feature maps, which we believe can be made more efficient. Hence on a single GeForce GTX 1080 GPU card, a standard GAE-p1 takes around 30 minutes to train for $100k$ steps, compared to 16 minutes for standard ConvAEs.